Electrochemistry Communications 121 (2020) 106874

Contents lists available at ScienceDirect

Electrochemistry Communications

journal homepage: www.elsevier.com/locate/elecom

Full Communication

Inactive materials matter: How binder amounts affect the cycle life of graphite electrodes in potassium-ion batteries

Fabian Jeschull *, Julia Maibach

Institute for Applied Materials – Energy Storage Systems (IAM-ESS), Karlsruhe Institute of Technology (KIT), Hermann-von-Helmholtz-Platz 1, 76344 Eggenstein-Leopoldshafen, Germany

ARTICLE INFO

Keywords:
Graphite electrode
Binder
Potassium-ion battery (PIB)
Capacity retention
CMC-Na
PAA

ABSTRACT

Recent results on the intercalation of potassium into graphite suggest that graphite might become yet again a negative electrode material of choice for an alkali-ion battery system. Compared to its mature application state in Li-ion batteries, graphite for K-ion applications is still in an early development stage. Although cycling of graphite-potassium half-cells over 200 cycles has been demonstrated, the electrodes clearly suffer from more severe capacity fading, as compared to the corresponding Li system. This study demonstrates that the capacity fade is strongly linked to the binder content in the composite electrode. High binder contents of 8 wt% (this study) or more (literature) show significant cycle life improvements over electrodes comprising of more practical binder contents of 4 wt% or less. The results highlight the need for revised or entirely new strategies to control the formation and stability of the electrode–electrolyte interphase in K-ion batteries.

1. Introduction

Graphite negative electrodes have been and still are the work horse in Li-ion battery research. To name but a few merits, graphite shows minor volume expansion during the Li-intercalation process (ca. 10%), low average intercalation potential, small voltage hysteresis, and a low surface area, making this active material an exceptionally stable negative electrode in comparison to alternative alloying or conversion materials [1,2]. In a similar fashion to Li-ions, graphite is capable to intercalate potassium-ions (K^+) into its host structure, thereby enabling its use as negative electrode in K-ion batteries (KIBs). In potassium cells, graphite exhibits an average potassiation potential of about 200 mV vs. K^+/K [3], a theoretical capacity of 279 mAh g^{-1} (KC_8) and a volume expansion of 60% in the fully potassiated state [4]. Literature reports up to 200 charge–discharge cycles in graphite-K-half-cells [4,5]. However, the cycle life is considerably shorter, the capacity fade stronger and the initial Coulombic efficiencies generally lower than in the case of Li-batteries. While part of these issues are rooted in the use of K-metal as counter electrode that is likewise a reactive component in the cell [6], there appear to be intrinsic shortcomings of the graphite electrode as well. As mentioned above, the graphite volume expansion is larger in case of potassium intercalation, putting additional stress on the stability of the solid-electrolyte interphase (SEI). Furthermore, the SEI products formed in a potassium half-cell are different from those formed in a lithium half-cell [7], a trend that has been reported previously also for Na-ion systems [8]. Improvements in the reversibility of graphite electrodes for KIBs have been demonstrated by Komaba and coworkers[9] who suggested the use of water-soluble binders such as carboxymethylcellulose sodium salt (CMC-Na) and sodium polyacrylate (PAA-Na), as compared to the conventional use of poly(vinylidene difluoride)-based (PVdF) binders. In fact, a literature survey (Table 1) shows that PVdF-based binders are the most commonly used binder materials in electrode formulations so far. In addition, it can be noted that the electrodes in these studies contained binder amounts of around 10 wt%, which is far from commercial standards [10]. Only two studies reported results on a graphite electrode formulations with less than 10 wt% binder [11,12].

This study also aims to work with a reduced, more practical binder content in graphite electrode formulations comparing their performance in LIBs and KIBs. As a result, a significant shortening of cycle life was observed that correlated with the binder content in the respective electrode formulation and appears to be a unique feature of the K-ion system. The results shed new light on the stability of the negative electrode in K-ion half-cell setups and are especially relevant for studies on K-ion full cells.

* Corresponding author.
E-mail address: fabian.jeschull@kit.edu (F. Jeschull).

https://doi.org/10.1016/j.elecom.2020.106874
Received 20 October 2020; Received in revised form 8 November 2020; Accepted 14 November 2020
Available online 23 November 2020

2. Experimental section

Graphite electrodes were prepared in batches of 2 g using a planetary mixer (Thinky, ARV-310P), following the weight ratios given in Table 2. A binder mixture comprising sodium carboxymethyl cellulose (CMC-Na, Merck) and polyacrylic acid (Merck, $M_v = 1.250$ kg mol^{-1}) in a 1:1 ratio by weight was prepared by dissolving the polymers in deionized water. The binder solution was blended with 1 wt% of carbon black (SuperC65, Imerys Graphite & Carbon, Switzerland) for 5 min at 2000 rpm. KS6L graphite (Imerys Graphite and Carbon, Switzerland) was added in two batches with a 5 min mixing (2000 rpm) for each batch. A total of 4.5 mL deionized water was used for the slurry. The slurry was cast with a doctor blade on copper foil, dried under ambient conditions and cut into discs of 14 mm in diameter (mass loadings: 2–3 mg_{AM} cm^{-1}). The electrodes and glassfiber separators (Whatman GF/B) were then dried at 120 °C overnight under vacuum. Cells were build as graphite-Li and graphite-K half-cells in a coin cell setup. One layer of glassfiber separator was soaked with 150 μL of an EC:DEC (v/v = 1:1, BASF) electrolyte mixture containing 750 mM $LiPF_6$ (battery grade, Merck) and KPF_6 (>99%, Merck) respectively. The salts were dried at 120 °C under vacuum overnight prior to use. The galvanostatic cycling tests were conducted on a Biologic VMP-3 potentiostat. The two initial cycles were conducted at C/20 (1C = 279 mA g^{-1} (K) and 372 mA g^{-1} (Li)) under constant-current constant-potential (CC-CP) conditions before the current density was increased to C/10. In addition, a time limit of 35 h was placed for the two initial cycles as safety precautionovercharge. The lower and upper cut-off voltages was chosen between 0.01 and 1.2 V vs. Li/Li^+ for Li half-cells and 0.025–1.2 V vs. K/K^+ for K half-cells.

3. Results and discussion

Our experimental series comprised of three different graphite electrode formulations containing 2, 4 or 8 wt% of a CMC-Na:PAA binder mixture, which were tested both in lithium and potassium half-cells. The electrolyte mixture was the same in both cases, except for the respective electrolyte salt. During drying, CMC-Na and PAA binder undergo crosslinking that has shown to be advantageous in electrode composites that contain expanding active material components [19,20]. In Fig. 1a-c the discharge capacities and corresponding coulombic efficiencies (C.E.) for the three formulations are shown in separate panels. Each panel contains the data for both the Li- and K-half-cells (lithium half-cell data are indicated in grey).

The results demonstrate that the graphite electrodes operate stably over the first 100 cycles independent of the binder content, when cycled in a Li-half-cell. Formulations comprising 4 wt% and 8 wt% binder exhibit discharge capacities of around 350 mAh g^{-1}. The electrode containing 2 wt% binder shows slightly higher discharge capacities of about 370 mAh g^{-1}. It is noteworthy, that the initial C.E. of around 79% (cycle #1) and 99% (cycle 2#) are approximately the same in all three cases. In contrast, in the corresponding potassium half-cells the same electrode formulations show significant differences in their respective cycle life. The 2 wt% binder composite reached a capacity retention of 50% after merely 50 cycles (Table 2). After another 50 cycles, the cell died completely. In comparison, the capacity retention after 50 cycles for the 4 wt% composite approached the 70% and the 8 wt% composite retained around 94% of its initial capacity. The differences are also reflected in the initial C.E. of the three formulations, summarized in Table 2: The initial C.E. improved from 48% to 71%, when the binder content is increased from merely 2 wt% to 8 wt%. The electrode with 4 wt% showed repeatedly fluctuations for different cells tested. The second cell in Fig. 1 (blue empty circles) displayed a capacity drop for 10 cycles before the capacity jumped back up, for reasons unknown. However, the general trend in capacity retention does not appear to be affected, by this temporary capacity drop.

When compared to the initial discharge capacities reported in literature (Table 1), the measured specific charge in this study for the 4 wt% (254 mAh g^{-1}) and 8 wt% (266 mAh g^{-1}) formulation are closer to the theoretical capacity of potassiated graphite than those reported in most previous works. Only the electrodes containing 2 wt% of the CMC-Na:PAA binder mixture showed a notably smaller specific charge (226 mAh g^{-1}) than the other two samples, which is partly attributed to the cut-off conditions on the first two cycles at C/20. Because of the high amount of irreversible charge, the first two cycles were not only limited by the cut-off voltage of 25 mV vs. K/K^+ but also by a time limit of 35 h, as a safety precaution against high pressure build-up due to gassing. While the charge process was finished for the 8 wt% formulation after about 28 h, both the 2 wt% and 4 wt% formulations reached the time limit before they reached the cut-off voltage (see also Fig. 2, cycle #01 and #02). This behaviour confirms the general trend that the irreversible charge loss is more severe the less binder is used in the electrode. A similar strong dependence between capacity retention and binder content is not known for the lithium system.

As previously mentioned, the K-metal counter electrode is a comparatively reactive component in K-half-cell setups and could by itself contribute significantly to detrimental side reactions that ultimately affect the performance of the working electrode as well [21]. It is therefore not surprising that generally lower C.E. are measured in K-systems. It is reasonable to assume that the K-metal electrode affects all cells equally, especially since the plating and stripping current densities at the K-metal counter electrode were similar because of similar active material loadings in all formulations. Therefore, even though K-metal certainly stands in the way of long cycle life in these half-cell tests, it is

Table 1
Previously reported electrode and performance parameters of graphite electrodes as negative electrodes in graphite-K half-cells. Included are studies employing graphite electrodes (excluding graphene or expanded graphite) and carbonate-based electrolytes. Entries until 2016 are also found in a review by Kim et al. [13]. A comprehensive overview of alternative carbon materials is provided in Ref. [14].

Reference	Year	Graphite, rel. amount	Binder, rel. amount	Electrolyte	1st cycle, $Q_{discharge}$/mAh g^{-1} (C.E.)	Estimated retention /mAh g^{-1} (#cycle)
Komaba et al. [9]	2015	Natural graphite (3 μm), 90 wt%	PVdF, 10 wt%	1 M KFSI, EC:DEC (1:1)	240 (59%)	220 (#20)
			CMC-Na, 10 wt%		230 (89%)	220 (#20)
			PAA-Na, 10 wt%		244 (79%)	225 (#50)
Jian et al. [15]	2015	SLP50, 90 wt%	PVdF, 10 wt%	0.8 M KPF_6, EC:DEC (1:1)	273 (57%)	110 (#50)
Luo et al. [16]	2015	NA[†], 80 wt%	PVdF, 20 wt%	0.5 M KPF_6, EC:DEC (1:1)	207 (74%)	–
Zhao et al. [4]	2016	KS4, 90 wt%	Na-alginate, 10 wt%	1 M KPF_6, EC:PC (1:1)	246 (66%)	220 (#100)
				1 M KPF_6, EC:DEC (1:1)	220 (46%)	210 (#100)
			PVdF, 10 wt%	1 M KPF_6, EC:PC (1:1)	240 (45%)	
An et al. [17]	2017	NA[†] ('commercial'), 80 wt%	CMC-Na, 10 wt%	1 M KFSI, EC:DEC (1:1)	202 (81%)	61 (#200)
Wang et al. [12]	2019	NA[†] ('synthetic'), 90 wt%	CMC-Na, 5 wt%	1 M KPF_6, EC:DMC(1:1)	135 (70%)	74 (#50)
Carboni et al. [5]	2019	SLP30, 90 wt%	KynarFlex 2801, 10 wt%	0.8 M KPF_6, EC:DEC (1:1)	211 (61%)	180 (#50)
Adams et al. [18]	2019	NA[†], 80 wt%	CMC-Na, 10 wt%	0.8 M KPF_6, EC:DEC (1:1)	300 (65%)	250 (#100)
Lei et al. [11]	2020	Natural graphite (7 m^2g^{-1}), 92 wt%	PVdF, 4 wt%	0.5 M KPF_6, EC:DEC (1:1)	240 (59%)	81 (#50)

[†] Type of graphite and manufacturer not further specified.

Table 2
Summary of the graphite electrode formulations and their respective performance parameters studied herein. The discharge capacities and C.E. refer to the mean value out of two measurements.

Binder content, wt.%	KS6L content, wt.%	Avg. areal mass loading, mg_{AM} cm^{-2}	Electrode porosity, % (±σ)	Discharge Capacities (Coulombic Efficiencies), $Q_{discharge}$/ mAh g^{-1} (C.E. / %)							
				Cycle #01		Cycle #02		Cycle #50		Cycle #75	
				K	Li	K	Li	K	Li	K	Li
2	97	2.64	56.3 (±1.7)	226.1 (47.6)	364.8 (79.4)	234.4 (85.6)	368.0 (99.1)	110.5 (26.6)	369.0 (100)	52.9 (22.2)	369.0 (100)
4	95	2.42	48.4 (±1.9)	254.3 (54.0)	340.6 (79.0)	264.9 (81.6)	343.6 (98.9)	194.6 (75.4)	344.5 (100)	180.6 (68.1)	344.4 (100)
8	91	2.22	50.6 (±1.8)	265.5 (71.3)	347.5 (79.3)	266.3 (91.7)	348.8 (98.9)	253.4 (95.0)	351.4 (100)	246.7 (93.7)	351.4 (100)

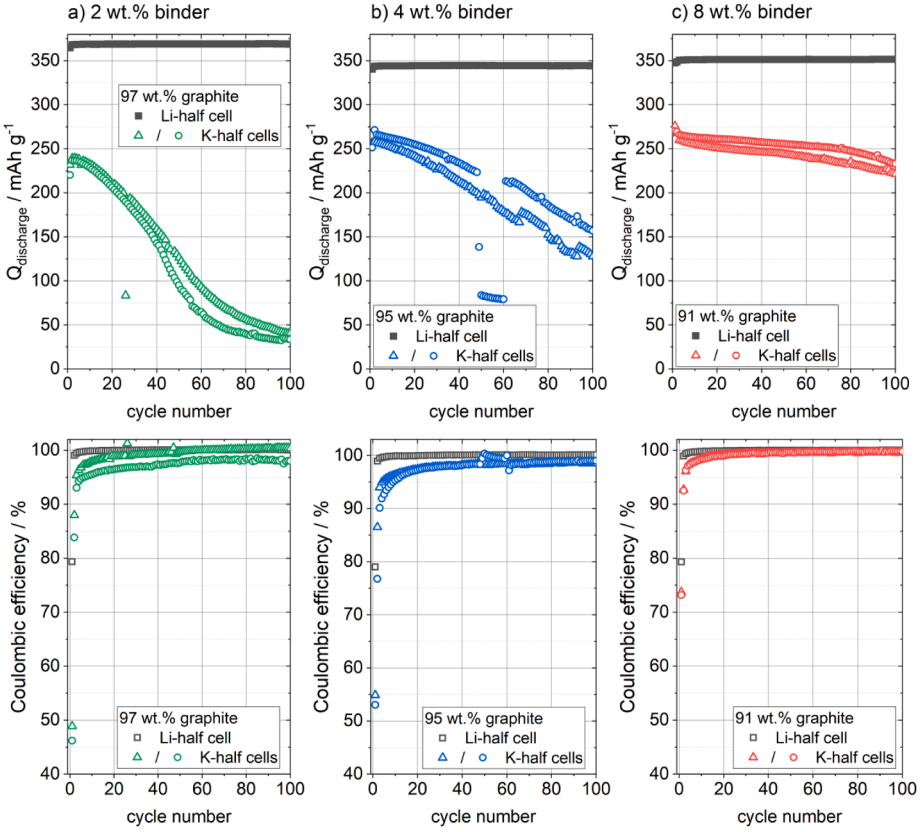

Fig. 1. Capacity retention (top row) and corresponding Coulombic efficiencies (C.E.; bottom row) of graphite electrodes with binder contents of 2 wt% (a), 4 wt% (b) and 8 wt% (c) examined in graphite-Li (grey squares) and graphite-K half-cells (coloured, two samples for each formulation).

unlikely to strongly interfere with the observed correlation between cycle life and binder content.

Shown in Fig. 2 are the voltage profiles for selected cycles for the three electrode formations examined in K-half-cells. The state-of-charge (SoC) is the charge q normalized by the specific capacity measured on the first potassiation. The potassiation is characterized by a sloping profile from 400 mV vs. K/K^+ onwards until a plateau is reached in the voltage range between 100 and 200 mV vs. K/K^+. On the basis of the voltage profiles of the first cycle (Cycle #01), a considerable irreversible charge contribution of about 20% of the whole charge transfer process is observed for the formulation with a 2 wt% binder content in the voltage region between OCV and 400 mV vs. K/K^+. This voltage region is characteristic for the SEI formation upon first charge. In the profile of the 2 wt% sample two regions between 1000 mV and 600 mV and from 600 mV to 400 mV can be distinguished that exhibit shallower slopes than electrodes with higher binder contents, indicating a larger extent of side reactions. Accordingly, electrodes comprising 4 wt% or 8 wt% binder display a steeper drop to the first intercalation potential, thus indicating a smaller degree of irreversible reactions. A comparison of the voltage profiles at different cycle numbers further shows that the electrodes suffer from a notable overpotential build-up over the first 50 cycles. While the onset of the lower intercalation plateau for the three samples was found on the first cycle at about 175 mV vs. K/K^+, it is located 75 mV vs. K/K^+ lower after only 50 cycles in case of an 8 wt% binder content. Using less binder increases the overpotential over this time even further. The position of the discharge plateau appears to be less affected over the same duration of the experiment. In the graphs for Cycle #01, #02 and #05, a local polarization maximum (indicated by black arrows in Fig. 2) is observed at the onset of the deintercalation reaction, which could indicate a kinetic hindrance at the beginning of the potassium extraction out of the graphite host structure. The feature disappears as the electrodes age.

For Li-ion batteries it is well known that the type of binder [22–24] as well as the binder coverage [25–28] has a profound impact on key

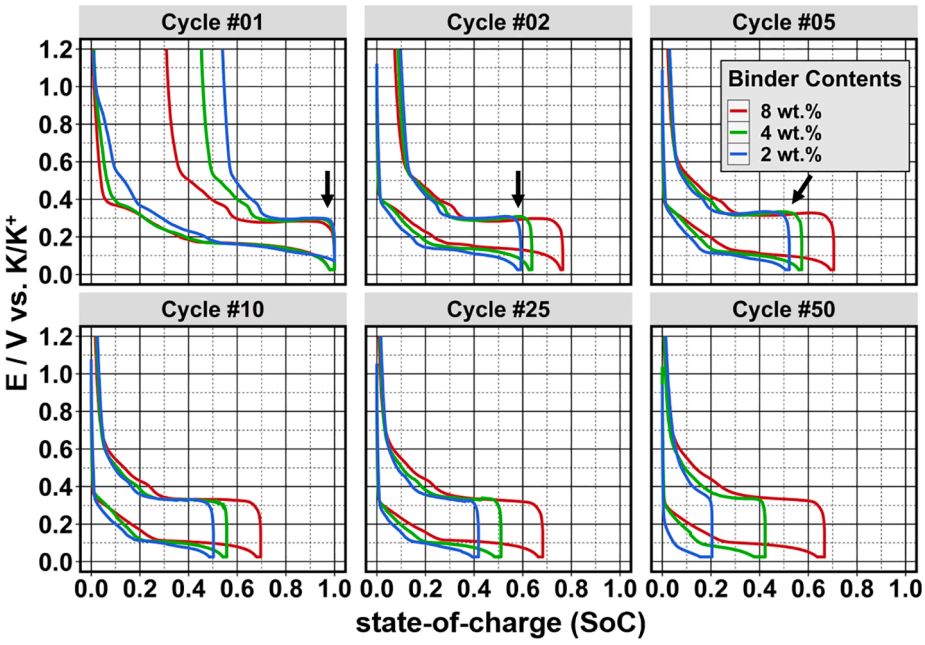

Fig. 2. Comparison between the voltage profiles of the three electrode formulations for selected cycles in K-half-cells. The black arrows indicate a polarization maximum at the beginning of deintercalation process.

performance parameters, such as the initial C.E. or capacity retention. Both CMC-Na and PAA are binders that swell poorly in carbonate solvents, contrary to common PVdF-based binders [25,29]. As such they may act as an intrinsic artificial SEI layer on the active material surface that is formed during slurry preparation and thus *prior* to any cycling. Binders can protect graphite particles from undesired side reactions, such as co-intercalation, and protect the electrode surface from direct contact with the electrolyte [24,25,30,31]. The latter depends decisively on the binder amounts and also its surfactant properties, as demonstrated for instance in a study by Karkar et al. [32] on Si electrodes that showed decreasing irreversible capacity losses (ICL) with increasing binder content. In addition, it is also reported that water-soluble binders tend to accumulate on the carbon black when the binder amounts are decreasing [25,26], leading to a depletion of polymer on the active material surface. Therefore, with respect to Li-ion systems it can be stated that both the type of binder and its amount in the electrode therefore alter the composition of the SEI layer [33–36]. This highlights how sensitive the electrode–electrolyte interface reacts to changes in its environment. Based on results reported on a comparison between SEI properties of Li- and Na-cells [8], SEI components formed in Li-containing electrolytes are less soluble and hence provide better surface protection. It might well be the case that SEI components formed in K-electrolytes suffer from similar solubility issues as their Na counterparts. Higher binder contents can partly mitigate this problem by providing a protective surface layer that is less prone to dissolution. In cases where the binder coverage is not sufficient, rapid capacity fade is imminent.

4. Conclusion

The results highlight that capacity fade is not a result of active material fatigue alone but may also depend on the choice of inactive components and the electrode composition. In particular, the binder content appears to be a parameter that should be chosen carefully when preparing graphite negative electrodes for K-ion batteries. Considering the promising results on K-ion full cells employing a graphite anode have already been reported [37], it is worth noting that the performance of such full cells is decisively determined by the reliability and stability of its anode. As an inactive component in an electrode, the binder lowers the energy density of a battery. However, in its role as an SEI component, binders may contribute to longer cycle life. Hence, for the further development of graphite-anode-based K-ion batteries, it will be paramount to find strategies to improve the key performance parameters at binder contents considerably lower than the currently used 10 wt%. The results further demonstrate that experiments on the same active material might lack a common basis for comparison between results of different studies, when the electrode compositions are different.

CRediT authorship contribution statement

Fabian Jeschull: Investigation, Formal analysis, Writing - original draft. **Julia Maibach:** Resources.

Declaration of Competing Interest

The authors declare that they have no known competing financial interests or personal relationships that could have appeared to influence the work reported in this paper.

Acknowledgements

This work contributes to the research performed at CELEST (Center for Electrochemical Energy Storage Ulm-Karlsruhe) and was funded by the German Research Foundation (DFG) under Project ID 390874152 (POLiS Cluster of Excellence).

References

[1] M.N. Obrovac, V.L. Chevrier, Chem. Rev. 114 (2014) 11444–11502.
[2] E.J. Berg, C. Villevieille, D. Streich, S. Trabesinger, P. Novák, J. Electrochem. Soc. 162 (2015) A2468–A2475.
[3] C. Vaalma, D. Buchholz, S. Passerini, Curr. Opin. Electrochem. 9 (2018) 41–48.
[4] J. Zhao, X. Zou, Y. Zhu, Y. Xu, C. Wang, Adv. Funct. Mater. 26 (2016) 8103–8110.
[5] M. Carboni, A.J. Naylor, M. Valvo, R. Younesi, RSC Adv. 9 (2019) 21070–21074.
[6] T. Hosaka, S. Muratsubaki, K. Kubota, H. Onuma, S. Komaba, J. Phys. Chem. Lett. 10 (2019) 3296–3300.
[7] A.J. Naylor, M. Carboni, M. Valvo, R. Younesi, ACS Appl. Mater. Interfaces 11 (2019) 45636–45645.
[8] R. Mogensen, D. Brandell, R. Younesi, ACS Energy Lett. 1 (2016) 1173–1178.
[9] S. Komaba, T. Hasegawa, M. Dahbi, K. Kubota, Electrochem. Commun. 60 (2015) 172–175.

[10] T. Marks, S. Trussler, A.J. Smith, D. Xiong, J.R. Dahn, J. Electrochem. Soc. 158 (2011) A51.
[11] Y. Lei, D. Han, J. Dong, L. Qin, X. Li, D. Zhai, B. Li, Y. Wu, F. Kang, Energy Storage Mater. 24 (2020) 319–328.
[12] L. Wang, J. Yang, J. Li, T. Chen, S. Chen, Z. Wu, J. Qiu, B. Wang, P. Gao, X. Niu, H. Li, J. Power Sources 409 (2019) 24–30.
[13] H. Kim, J.C. Kim, M. Bianchini, D.-H. Seo, J. Rodriguez-Garcia, G. Ceder, Adv. Energy Mater. 8 (2018) 1702384.
[14] Y. Wu, H. Zhao, Z. Wu, L. Yue, J. Liang, Q. Liu, Y. Luo, S. Gao, S. Lu, G. Chen, X. Shi, B. Zhong, X. Guo, X. Sun, Energy Storage Mater. 34 (2021) 483–507.
[15] Z. Jian, W. Luo, X. Ji, J. Am. Chem. Soc. 137 (2015) 11566–11569.
[16] W. Luo, J. Wan, B. Ozdemir, W. Bao, Y. Chen, J. Dai, H. Lin, Y. Xu, F. Gu, V. Barone, L. Hu, Nano Lett. 15 (2015) 7671–7677.
[17] Y. An, H. Fei, G. Zeng, L. Ci, B. Xi, S. Xiong, J. Feng, J. Power Sources 378 (2018) 66–72.
[18] R.A. Adams, A. Varma, V.G. Pol, J. Power Sources 410–411 (2019) 124–131.
[19] B. Koo, H. Kim, Y. Cho, K.T. Lee, N.-S. Choi, J. Cho, Angew. Chem. Int. Ed. 51 (2012) 8762–8767.
[20] Y. Surace, F. Jeschull, T. Schott, S. Zürcher, M.E. Spahr, S. Trabesinger, ACS Appl. Energy Mater. 2 (2019) 7364–7374.
[21] L. Madec, V. Gabaudan, G. Gachot, L. Stievano, L. Monconduit, H. Martinez, ACS Appl. Mater. Interfaces 10 (2018) 34116–34122.
[22] F. Jeschull, D. Brandell, M. Wohlfahrt-Mehrens, M. Memm, Energy Technol. 5 (2017) 2108–2118.
[23] H. Buqa, M. Holzapfel, F. Krumeich, C. Veit, P. Novák, J. Power Sources 161 (2006) 617–622.
[24] S. Komaba, T. Ozeki, K. Okushi, J. Power Sources 189 (2009) 197–203.
[25] F. Jeschull, M.J. Lacey, D. Brandell, Electrochim. Acta 175 (2015) 141–150.
[26] T. Nordh, F. Jeschull, R. Younesi, T. Koçak, C. Tengstedt, K. Edström, D. Brandell, ChemElectroChem 4 (2017) 2683–2692.
[27] K.A. Hirasawa, K. Nishioka, T. Sato, S. Yamaguchi, S. Mori, J. Power Sources 69 (1997) 97–102.
[28] S. Fukuyama, H. Oji, S. Yasuno, S. Komaba, ACS Sustainable Chem. Eng. 5 (2017) 6343–6355.
[29] A. Magasinski, B. Zdyrko, I. Kovalenko, B. Hertzberg, R. Burtovyy, C.F. Huebner, T. F. Fuller, I. Luzinov, G. Yushin, ACS Appl. Mater. Interfaces 2 (2010) 3004–3010.
[30] S. Komaba, K. Okushi, T. Ozeki, H. Yui, Y. Katayama, T. Miura, T. Saito, H. Groult, Electrochem. Solid-State Lett. 12 (2009) A107.
[31] F. Jeschull, D. Brandell, K. Edström, M.J. Lacey, Chem. Commun. 51 (2015) 17100–17103.
[32] Z. Karkar, D. Guyomard, L. Roué, B. Lestriez, Electrochim. Acta 258 (2017) 453–466.
[33] F. Jeschull, J. Maibach, R. Félix, M. Wohlfahrt-Mehrens, K. Edström, M. Memm, D. Brandell, ACS Appl. Energy Mater. 1 (2018) 5176–5188.
[34] F. Jeschull, J. Maibach, K. Edström, D. Brandell, J. Electrochem. Soc. 164 (2017) A1765–A1772.
[35] S. Leroy, F. Blanchard, R. Dedryvère, H. Martinez, B. Carré, D. Lemordant, D. Gonbeau, Surf. Interface Anal. 37 (2005) 773–781.
[36] L. El Ouatani, R. Dedryvère, J.-B. Ledeuil, C. Siret, P. Biensan, J. Desbrières, D. Gonbeau, J. Power Sources 189 (2009) 72–80.
[37] X. Bie, K. Kubota, T. Hosaka, K. Chihara, S. Komaba, J. Mater. Chem. A 5 (2017) 4325–4330.